JEM

# Supplemental material

Chen et al., https://doi.org/10.1084/jem.20171767

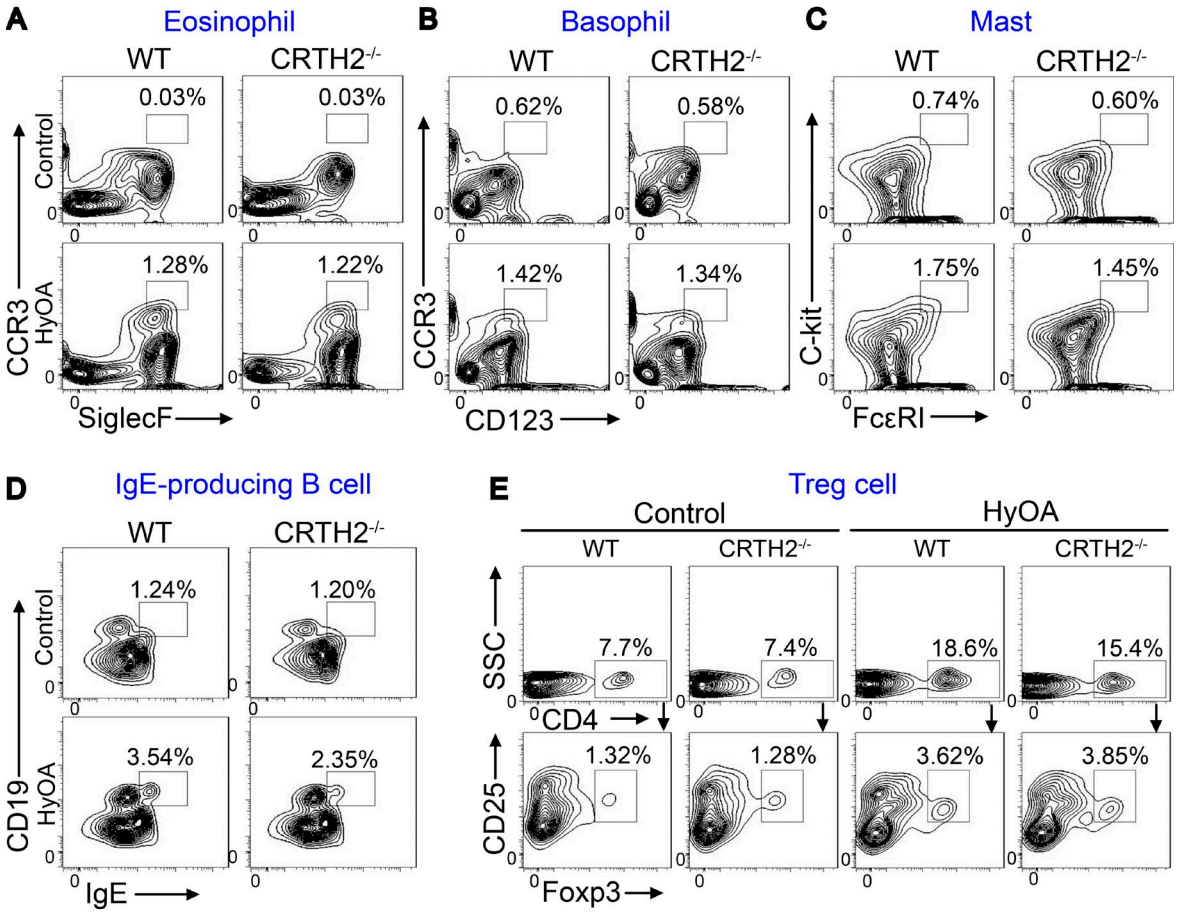


F

| Cell Type | Group | Control | | HyOA | |
|---|---|---|---|---|---|
| | | WT | CRTH2$^{-/-}$ | WT | CRTH2$^{-/-}$ |
| Lung | Eosinophil (%) | 0.04±0.01 | 0.03±0.01 | 1.26±0.12$^{\#}$ | 1.22±0.03$^{\#}$ |
| | Basophil (%) | 0.64±0.05 | 0.59±0.04 | 1.43±0.06$^{\#}$ | 1.36±0.04$^{\#}$ |
| | Mast cell (%) | 0.72±0.06 | 0.58±0.05 | 1.74±0.04$^{\#}$ | 1.42±0.11$^{*,\#}$ |
| | B cell (%) | 1.26±0.09 | 1.17±0.07 | 3.45±0.18$^{\#}$ | 2.31±0.20$^{*,\#}$ |
| | Treg(%) | 1.34±0.08 | 1.25±0.07 | 3.64±0.19$^{\#}$ | 3.82±0.28$^{\#}$ |
| BALF | Eosinophil (%) | 0.42±0.03 | 0.33±0.03 | 2.32±0.10$^{\#}$ | 2.20±0.22$^{\#}$ |
| | Basophil (%) | 0.43±0.03 | 0.50±0.03 | 2.44±0.06$^{\#}$ | 2.36±0.17$^{\#}$ |
| | Mast (%) | 1.42±0.09 | 1.37±0.07 | 4.25±0.22$^{\#}$ | 2.75±0.12$^{*,\#}$ |
| | B cell (%) | 1.24±0.08 | 1.34±0.06 | 4.34±0.27$^{\#}$ | 3.50±0.38$^{*,\#}$ |
| Blood | Eosinophil (%) | 0.83±0.04 | 0.73±0.05 | 2.38±0.08$^{\#}$ | 2.41±0.15$^{\#}$ |
| | Basophil (%) | 0.27±0.01 | 0.31±0.02 | 1.58±0.11$^{\#}$ | 1.74±0.10$^{\#}$ |
| | Mast cell (%) | 0.46±0.03 | 0.50±0.02 | 2.28±0.10$^{\#}$ | 1.79±0.14$^{*,\#}$ |
| | B cell (%) | 1.23±0.08 | 1.28±0.08 | 6.43±0.34$^{\#}$ | 3.34±0.20$^{*,\#}$ |

Figure S1. **Effect of CRTH2 deficiency on Th2 response-associated cell response in lung tissue, BALF, and peripheral blood in HyOA-induced mice. (A–E)** Representative flow cytometry charts of the frequency of eosinophils (CCR3$^+$SiglecF$^+$; A), basophil (CCR3$^+$CD123$^+$; B), mast cells (c-kit$^+$FcεRI$^+$; C), IgE-producing B cells (CD19$^+$IgE$^+$; D), and T reg cells (CD4$^+$CD25$^+$FoxP3$^+$; E) in lung tissues of HyOA-treated mice. **(F)** Quantification of the frequency of eosinophils, basophils, mast cells, IgE-producing B cells, and T reg cells in lung tissues, BALF, and peripheral blood of HyOA-treated WT and CRTH2$^{-/-}$ mice. *n* = 6–8 mice per group. *, P < 0.05 versus WT; #, P < 0.05 versus control. All graphs are shown as mean ± SEM. Data are representative of at least two independent experiments. Statistical significance was determined using two-way ANOVA followed by a Bonferroni post hoc test and unpaired Student's *t* tests.

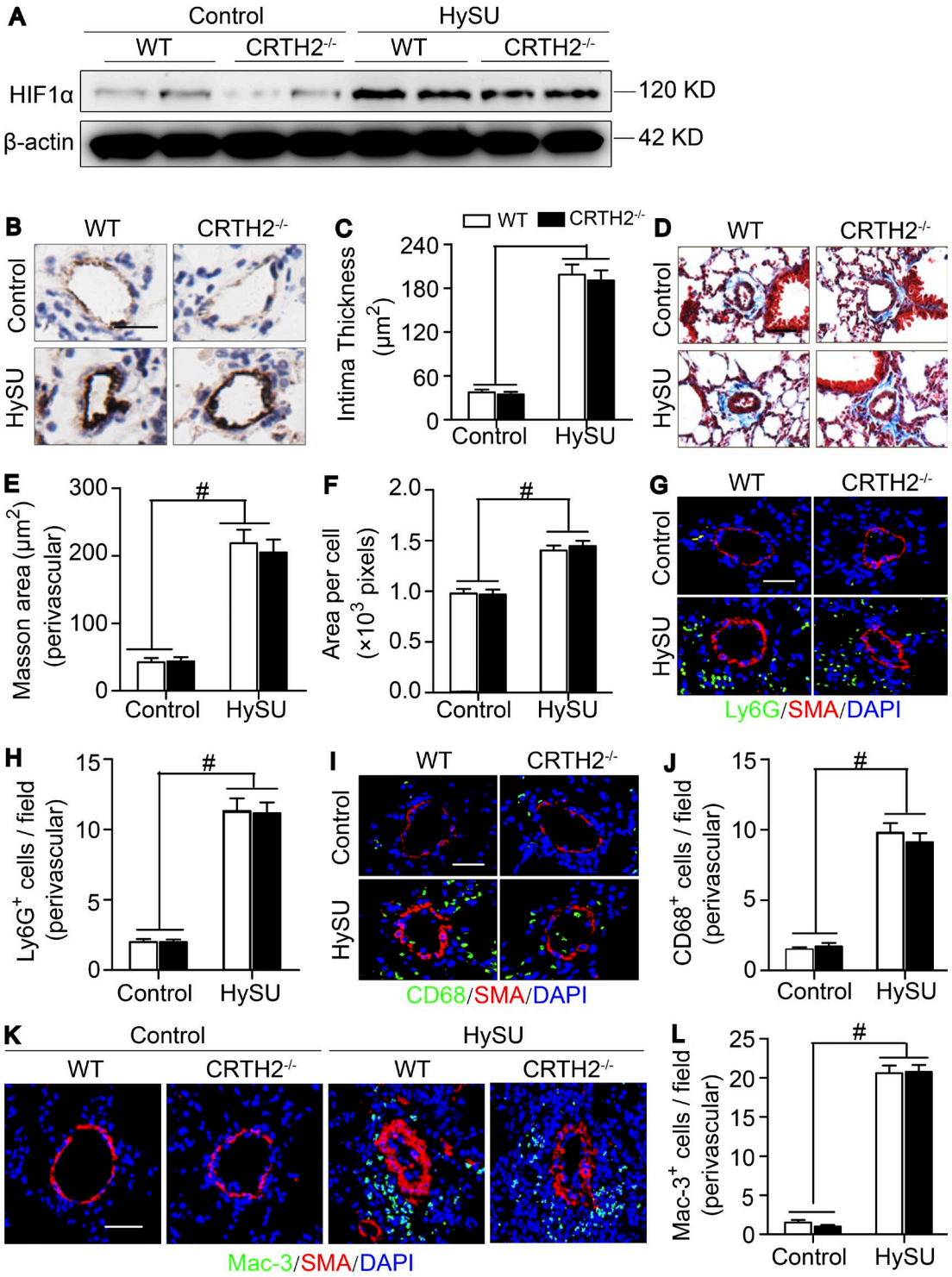


Figure S2. **Pathological characterization of HySU-induced PAH in CRTH2$^{-/-}$ mice. (A)** Western blot analysis of HIF-1α protein level in lung tissues of HySU-induced mice. **(B)** Representative images of immunohistochemical staining of von Willebrand factor in lung tissues from HySU-treated WT and CRTH2$^{-/-}$ mice. Bar, 20 µm. **(C)** Quantification of the thickness of the intima of PAs by Image-Pro Plus in B. **(D)** Representative images of Masson's trichrome staining of lung tissues from HySU-treated WT and CRTH2$^{-/-}$ mice. Bar, 20 µm. **(E)** Quantification of the perivascular collagen area in D by Image-Pro Plus. **(F)** Quantification of cell size of PASMCs in PAs from HySU-treated WT and CRTH2$^{-/-}$ mice. **(G)** Representative images of Ly6G immunostaining of lung sections from HySU-treated mice. Bar, 20 µm. **(H)** Quantification of neutrophils (Ly6G$^{+}$ cells) in perivascular areas shown in G. **(I)** Representative images of CD68 immunostaining of lung sections from HySU-treated mice. Bar, 20 µm. **(J)** Quantification of macrophage (CD68$^{+}$ cells) in perivascular areas shown in I. **(K)** Representative images of Mac-3 immunostaining of lung sections from HySU-treated mice. Bar, 20 µm. **(L)** Quantification of macrophage (Mac-3$^{+}$ cells) in perivascular areas shown in K. In A–K, $n$ = 8–10 mice per group. #, $P < 0.05$ as indicated. All data are expressed as mean ± SEM and are representative of at least two independent experiments. Statistical significance was determined using two-way ANOVA followed by a Bonferroni post hoc test and unpaired Student's $t$ tests.

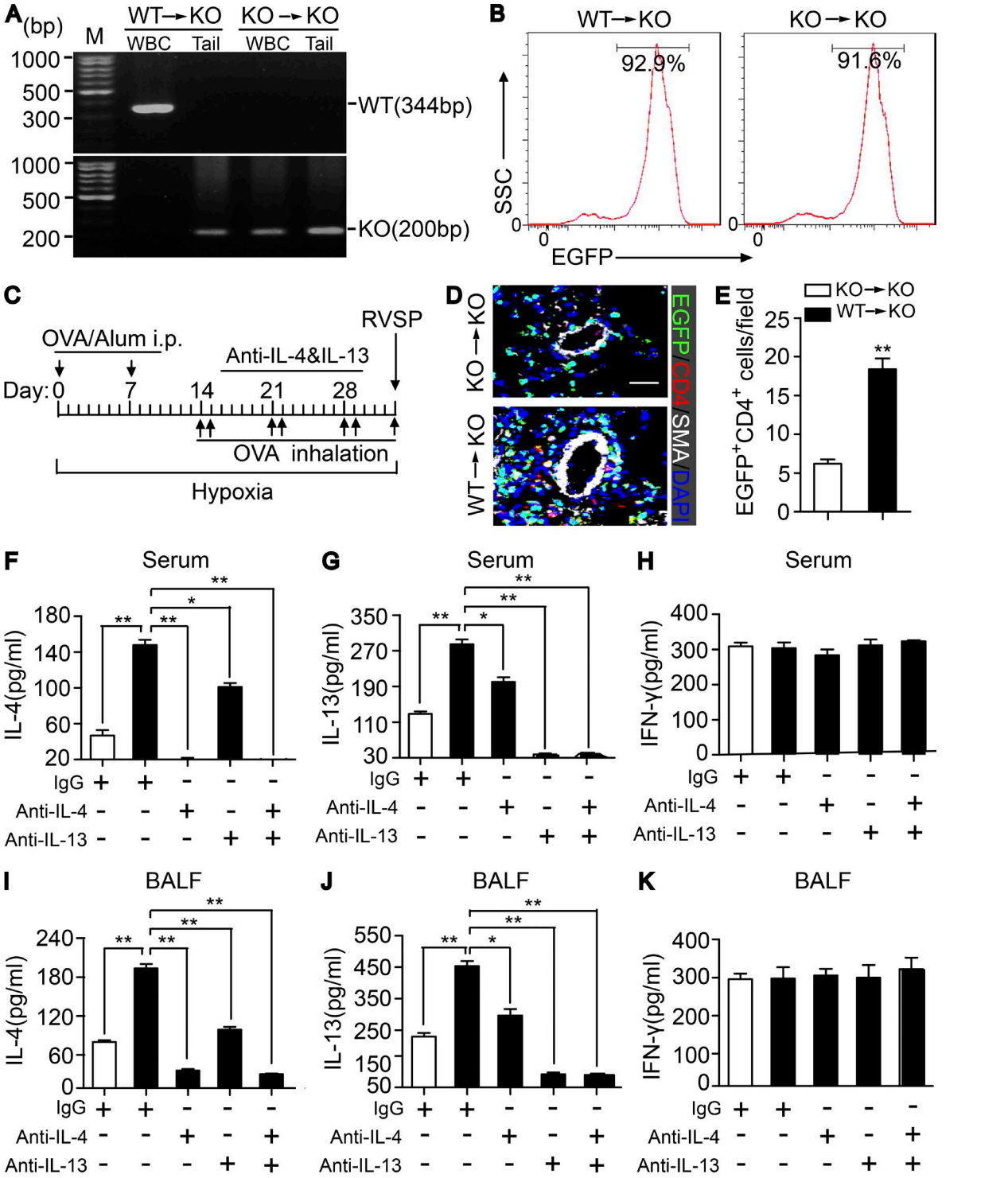


Figure S3. **CRTH2$^{+/+}$ BM reconstruction enhances Th2 immune response in the lungs in HyOA-treated CRTH2$^{-/-}$ mice. (A)** Confirmation of BMT by means of genotyping. **(B)** The efficacy of BM reconstitution in CRTH2$^{-/-}$ mice by flow cytometry. **(C)** Schematic representation of the protocol for administration of BM-reconstructed mice to induce PAH. **(D)** Representative immunofluorescence images of EGFP (green), CD4 (red), and SMA (white) in lung tissues from BM-reconstructed mice. Bar, 20 µm. **(E)** Quantification of perivascular EGFP$^{+}$CD4$^{+}$ cells in lung tissues from BM-reconstructed mice as shown in D. **(F–K)** Quantification of IL-4 (F and I), IL-13 (G and J), and IFN-γ (H and K) levels in the serum (F–H) and BALF (I–K) from HyOA-treated KO→KO and WT→KO mice with or without dual neutralization of IL-4 and IL-13. In A–K, $n$ = 8–10 mice per group. *, P < 0.05; **, P < 0.01 as indicated. Representative data are shown as mean ± SEM derived from at least two independent experiments. Statistical significance was determined using unpaired Student's $t$ tests. SSC, side scatter; WBC, white blood cell.

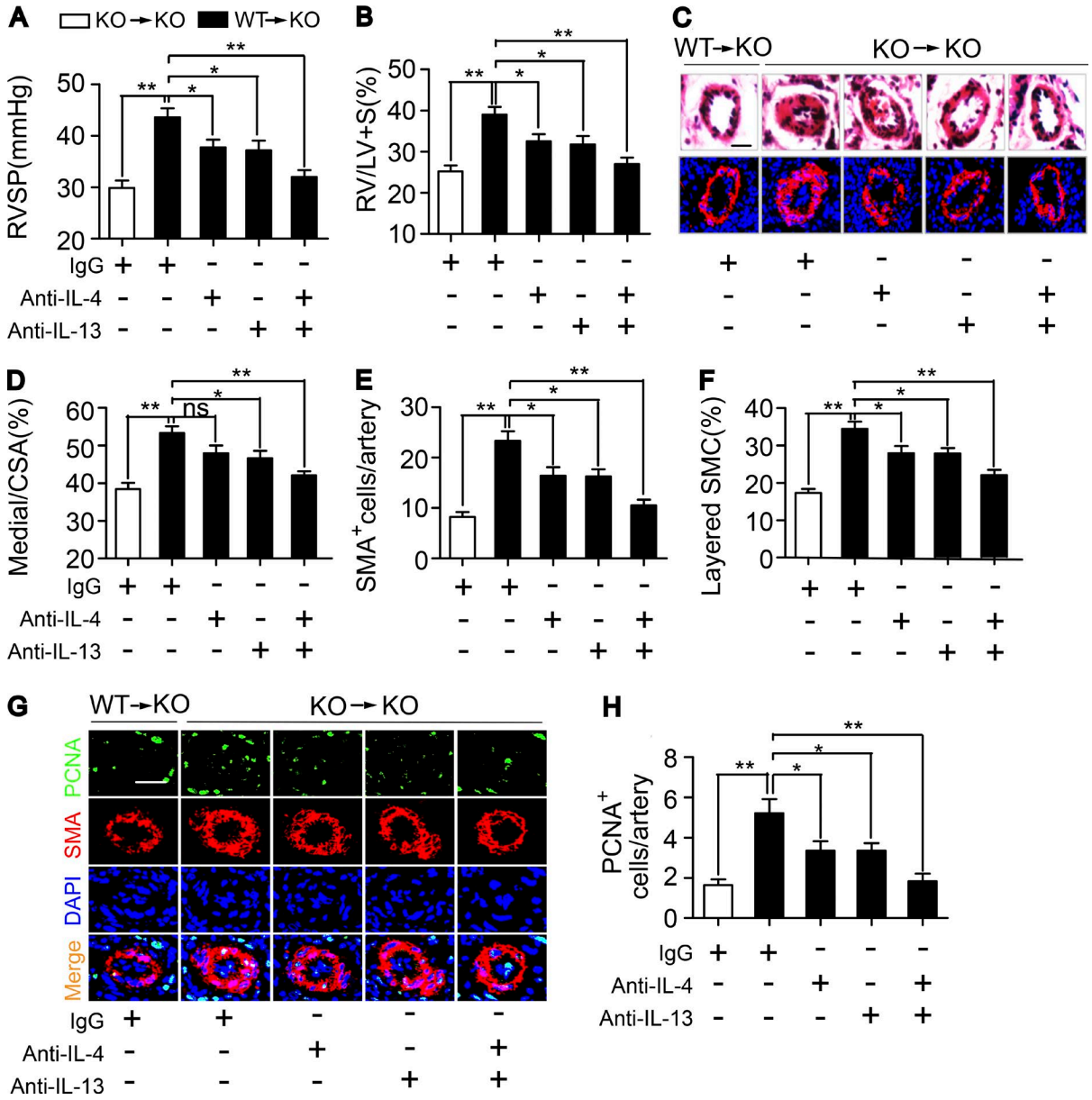


Figure S4. **CRTH2$^{+/+}$ BMT aggravates HyOA-induced PAH in CRTH2$^{-/-}$ mice by increasing IL-4 and IL-13 secretion. (A and B)** Effect of CRTH2$^{+/+}$ BMT on RVSP (A) and RV/LV + S ratio (B) in HyOA-treated CRTH2$^{-/-}$ mice with or without dual neutralization of IL-4 and IL-13. **(C)** Representative images of H&E staining and SMA (red) immunostaining of PAs of BM-reconstituted mice with or without dual neutralization of IL-4 and IL-13. Bar, 20 µm. **(D)** Quantification of the ratio of pulmonary arterial medial thickness to total vessel size (media/CSA) for the BM-reconstructed mice. **(E and F)** Quantification of the number (E) and percentages (F) of layered SMCs in PAs from BM-reconstructed mice. **(G)** Representative PCNA (green) and α-SMA (red) immunostaining of lung sections from BM-reconstructed mice. Bar, 20 µm. **(H)** Quantification of PCNA$^{+}$ cells in PAs. In A–H, $n$ = 8–10 mice per group. *, P < 0.05; **, P < 0.01 as indicated. All data are shown as mean ± SEM and are representative of at least two independent experiments. Statistical significance was determined using unpaired Student's *t* tests.

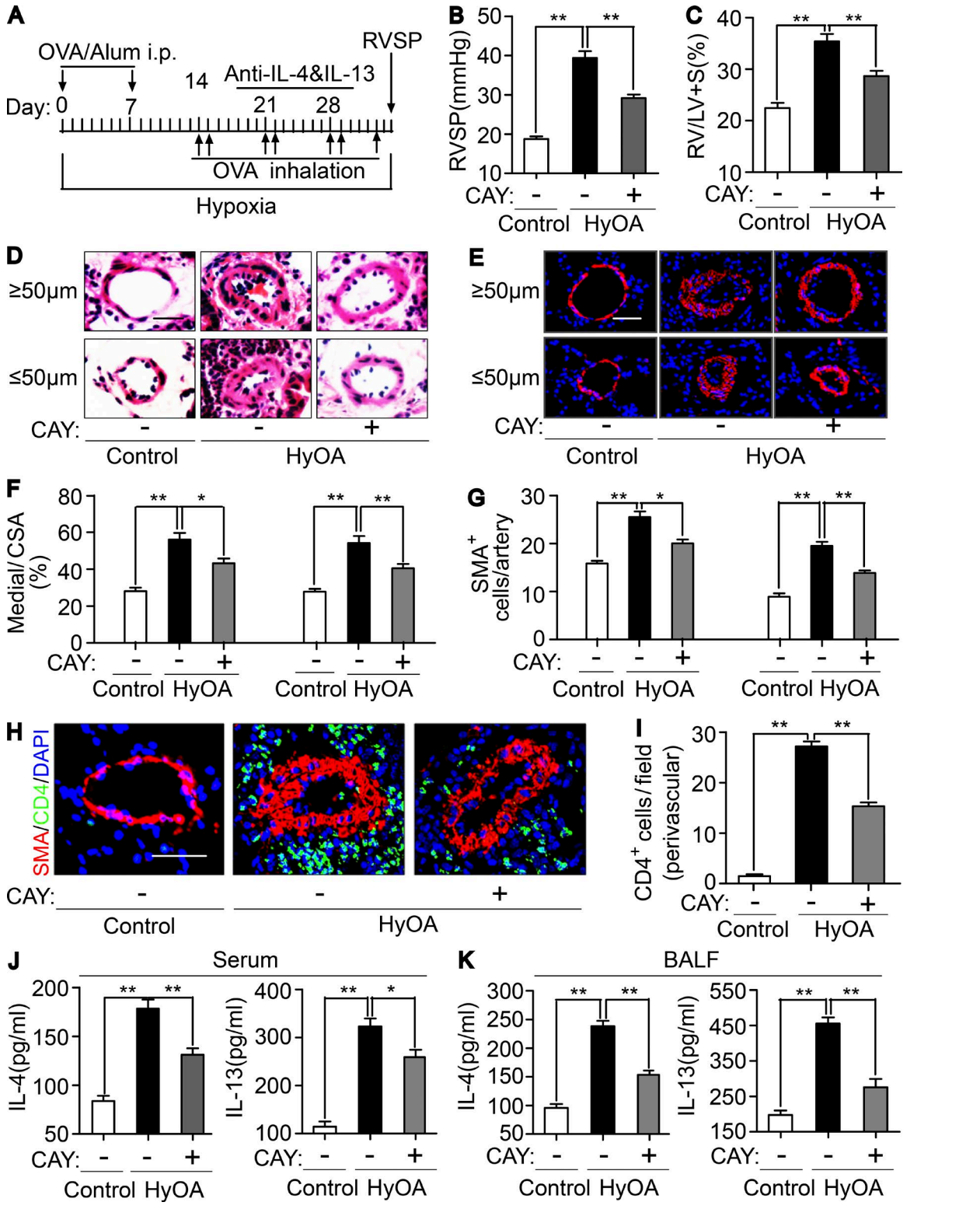


Figure S5. **Pharmacological inhibition of CRTH2 ameliorates HyOA-induced PAH in mice. (A)** Protocol for administration of CRTH2 inhibitor CAY10595 to HyOA-challenged mice. **(B and C)** Effect of CAY10595 administration on RVSP (B) and RV/LV + S ratio (C) of HyOA-treated mice. CAY, CAY10595. **(D and E)** Representative images of H&E staining (D) and SMA (red) immunostaining (E) of lung sections of HyOA-challenged mice treated with CAY10595 or equivalent volume of vehicle. Bars, 20 µm. **(F and G)** Quantification of the ratio of pulmonary arterial medial thickness to total vessel size (media/CSA; F) and the number of SMA$^+$ cells in PAs (G) from HyOA-challenged mice with CAY10595 treatment. **(H)** Representative images of CD4 (green) and SMA (red) immunostaining of lung tissues from HyOA-challenged mice treated with CAY10595. Bar, 20 µm. **(I)** Quantification of perivascular infiltration of CD4$^+$ cells in the lungs in HyOA-challenged mice after CAY10595 treatment. **(J and K)** Quantification of secretion levels of IL-4 and IL-13 in the serum (J) and BALF (K) from HyOA-challenged mice after CAY10595 treatment. In A–K, $n$ = 10–12 mice per group. *, $P < 0.05$; **, $P < 0.01$ as indicated. Data are presented as mean ± SEM derived from at least two independent experiments. Statistical significance was determined using unpaired Student's $t$ tests.